

Robust VF and PQ Control of a Photovoltaic System Connected to Grid with Battery Storage Management

Abstract. This paper presents an advanced control of photovoltaic system with battery storage system and shows the coordination of the studied system in order to enhance solar energy utilization. This study proposes an approach of coordinated and integrated control of solar PV generators with battery storage control in order to maintain active and reactive power (P-Q) control and to provide voltage and frequency (V-f) support to the grid instead of a high load addition. The description of the studied system is based on a battery energy storage system based (lithium-ion technology), a DC-DC bidirectional power converter in order to connect the battery to the DC bus, DC-DC converter, voltage source inverter and finally the load and the micro-grid. Consequently, the main contribution of the proposed control methods lies in the coordination between the different controls methods proposed: battery control at the PV side and V-f/P-Q control algorithm at the inverter side. A simulation using the Matlab/Simulink software has been performed, to confirm that the proposed control model is able to provide voltage and frequency support to the grid and to maintain active and reactive power control instead of a high load addition.

Streszczenie. Niniejszy artykuł przedstawia zaawansowaną kontrolę systemu fotowoltaicznego z systemem baterii i pokazuje koordynację badanego systemu w celu zwiększenia wykorzystania energii słonecznej. W opracowaniu zaproponowano podejście polegające na skoordynowanym i zintegrowanym sterowaniu generatorami fotowoltaicznymi z kontrolą akumulatorów w celu utrzymania kontroli mocy czynnej i biernej (P-Q) oraz zapewnienia wsparcia napięcia i częstotliwości (V-f) dla sieci zamiast dodawania wysokiego obciążenia. Opis oparty jest na systemie akumulacji energii akumulatora (technologia litowo-jonowa), dwukierunkowym konwerterze mocy DC-DC w celu podłączenia akumulatora do szyny DC, przetwornicy DC-DC, falownika źródła napięcia i wreszcie obciążenie. W związku z tym główny wkład proponowanych metod sterowania polega na koordynacji różnych proponowanych metod sterowania: kontrolą baterii po stronie PV i algorytm sterowania V-f / P-Q po stronie falownika. Przeprowadzono symulację za pomocą oprogramowania Matlab / Simulink, aby potwierdzić, że proponowany model sterowania jest w stanie zapewnić wsparcie napięcia i częstotliwości dla sieci oraz utrzymać kontrolę mocy czynnej i biernej zamiast dodatku o wysokim obciążeniu. (Solidne sterowanie VF i PQ systemu fotowoltaicznego podłączonego do sieci z zarządzaniem akumulatorami).

Keywords: Active and reactive power control; Battery energy storage; PV System; Voltage and frequency control.

Słowa kluczowe: Kontrola mocy czynnej i biernej; Magazynowanie energii baterii; System PV; Regulacja napięcia i częstotliwości.

1. Introduction

Nowadays, the development of power electronics has resulted in more powerful and more responsive power converters, which make it possible to control complex distributed generators and various functions of the energy storage management system [1]–[3]. However, integrating renewable energy production into existing electricity network generates serious problems, such as the variability and intermittency of the resources that influence the stability of the grid, moreover, it creates also a difference between electricity demand and renewable energy sources production, to avoid such a problem and to take full advantage of renewable energies, storage technologies are increasingly discussed as one of the main means to ensure the security of electricity supply in the future. For this reason Battery Energy Storage System (BESS) are one of the necessary solutions for integrating renewable energy production into existing electricity network [4]. To harness the BESS technology, an operation and control of the inverter interface of renewable energy should be provided and it's a real challenge, especially when it comes to maintaining both micro grid voltage and frequency within an acceptable range.

This paper presents a control of photovoltaic system with the maximum power tracking and the battery storage control in order to provide voltage and frequency support to the grid and to maintain active and reactive power control instead of high load addition. However, there are not many research has been done on V-f and P-Q control using solar PV including battery storage. For example in [5], frequency regulation with PV in micro grid is studied; however, this work does not consider the voltage control objective and lacks battery storage in the micro grid, as well as in [6], the proposed model doesn't consider the addition of high load, also in [7], frequency control is implemented in micro grid PV and storage; however, this work also lacks the consideration of a voltage control objective. This study proposes an approach of coordinated and integrated control of solar PV generators with battery storage system in order

to maintain active and reactive power (P-Q) control and to provide voltage and frequency (V-f) support to the grid, for this reason detailed models of PV, battery, converter and inverter are developed and the proposed structure consists of two-conversion system: a DC-DC boost converter and a voltage source inverter. The DC-DC boost converter boosts the actual voltage at the maximum power point to a constant value which equal to $V_{DC} = 500V$, moreover, this converter is controlled by the maximum power point tracking (MPPT) algorithm based on the Perturb and Observe technique (P&O) [8]–[10]. In order to connect the PV panel and the DC-DC converter to the grid we need a voltage source inverter [11], [12], and finally the system is connected to grid.

The utility grid serves as the main source when the power generated by photovoltaic panel as well as the battery power is not available or as a complementary source in the case when the power generated by both systems is not sufficient to satisfy the load. The major contribution of the proposed control methods lies in the coordination between the different controls methods proposed: battery control at the PV side and V-f / P-Q control algorithm at the inverter side. These control algorithms are suitably connected to the DC and AC sides of the inverter, so that the DC side voltage is controlled indirectly to the desired value in order to maintain the AC side voltage at the desired voltage. In addition, the proposed control methods have the ability to manage the state of charge (SOC) constraints and specially to provide voltage and frequency (V-f) support to the grid instead of load addition and this is the main idea that we develop in the rest of this study.

The rest of this paper is organized as follows: Section 3 presents a description on the studied system. Section 4; develop the overall control schemes for both battery integrated V-f and P-Q control. Then, the obtained results using Matlab/Simulink are presented in Section 5. Finally, conclusion is giving in Section 6.

II. Notation

The notation used throughout the paper is stated below:

- $v_1(t)$: Instantaneous PCC voltage
- $V_1(t)$: Average PCC voltage
- $v_c(t)$: Instantaneous inverter output voltage
- $V_c(t)$: Average inverter output voltage
- $P(t)$: Inverter active power
- $Q(t)$: Inverter reactive power
- $S(t)$: Inverter apparent power
- P_{pv} : PV active output power
- α_1^* : Phase shift between $v_c(t)$ and $v_1(t)$
- δ^* : Duty cycle of DC/DC boost
- f_{ref} : Reference micro grid frequency
- f : Measured micro grid frequency
- P_{AC} : AC side total active power
- P_{DC} : DC side total active power
- P_B : Actual injected battery active power
- P_{Bref} : Reference battery active power
- Q : Actual generated reactive power
- Q_{ref} : Reference reactive power
- P : Actual generated reactive power
- P_{ref} : Reference active power

III. PV system configuration

Figure 1 shows the topology of the modelled system with PV operating at Maximum Power Point (MPP). Where the DC-DC boost converter is used for MPPT control, battery storage system is connected in parallel to the PV to inject and absorb power through a bidirectional DC-DC converter and at least the PV system is connected to the grid by means of DC-AC converter [13]–[15].

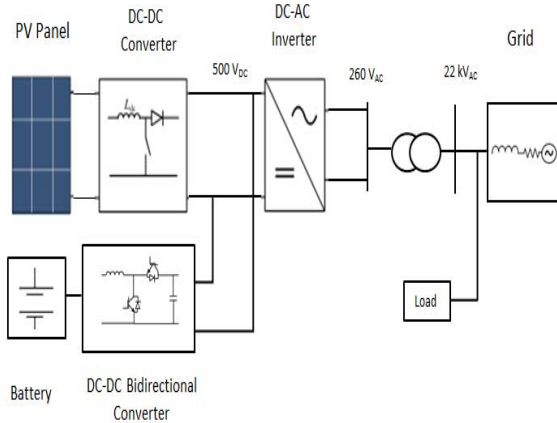


Fig. 1. Topology of the modelled system

III.1. PV Panel

A single diode model with both series and parallel resistors models the PV array; the equivalent circuit is giving by the following figure [16]:

The PV circuit model is based on the following equation [17]:

$$(1) \quad I = I_{pv} - I_0 \left[\exp \left(\frac{V + R_s \times I}{V_t \times A} \right) - 1 \right] - \left(\frac{V + R_s \times I}{R_p} \right)$$

where: I_{pv} - photoelectric current (9A); I_0 - diode saturation current (A); V_t - junction thermal voltage

$\left[V_t = \frac{k.T}{q} \right]$; q - electron charge $[1.602 \times 10^{19} C]$; k - Boltzman constant $[1.38 \times 10^{22} J / K]$; T - cell temperature (9K); V - thermal voltage (9V); R_s - cell series resistance (Ω); R_p - cell shunt resistance (Ω); A - diode ideality factor.

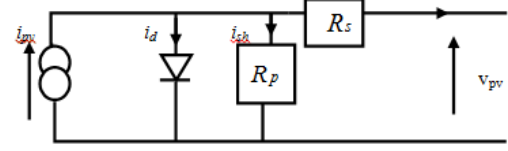


Fig. 2. Single diode model of the PV

The principal specifications for this model are given in Table I (Appendix).

The PV panel used in this study consists of 66 strings of 5-series-connected modules connected in parallel, which creates a photovoltaic plant with nominal output power of 100.7 kW and voltage of 273.5 V at the maximum power point [18].

III.2. Battery Energy Storage System (BESS)

Battery is a group of electrochemical cells which convert chemical energy into electrical energy [19], [20]. The BESS used in this study consists of lithium-ion batteries connected to bidirectional DC-DC converter. Typical discharge characteristic is shown in Figure 3, the battery nominal voltage and discharge current is 260V, 260A. A nominal output power of 67.7kW is obtained by these values; the rated capacity is 3000 Ah.

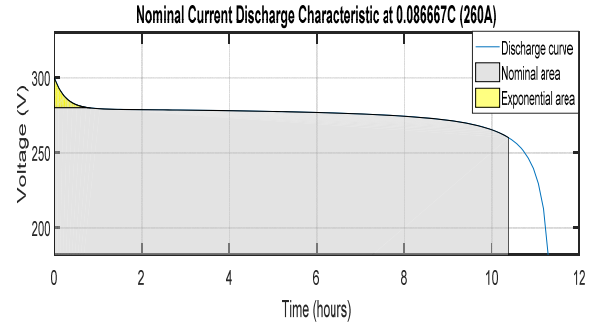


Fig. 3. Nominal current discharge characteristic at 0.087 C

The BESS is connected to bidirectional DC-DC converter that allows the current to flow in both directions. The bidirectional converter charges or discharges the battery according to the power request. The required power is obtained by the following equation that describes the active power balance between the production and the consumption side:

$$(2) \quad P_{pv} + P_{batt} = P_{load} + \Delta P$$

where: P_{batt} - the required power from the battery; P_{pv} - the power generated by the photovoltaic panel; ΔP - power losses.

This equation result is fed to bidirectional DC-DC converter as a required power command.

IV. Battery integrated V-F and P-Q control

Figure 4 shows the PV system configuration for V-f and P-Q control, it contains a battery system which is connected

in parallel to the PV system in order to inject or absorb power through a bidirectional DC-DC converter.

When the battery is injecting power to the grid, the converter operates in the boost mode and when the battery is absorbing power, it operates in the buck mode. The operation mode is controlled through the control signal provided to the converter switches.

The PV system is connected to the grid through a coupling inductor L_c . The coupling inductor filters out the ripples in the PV output current. The connection point is called the point of common coupling (PCC) and the PCC voltage is denoted as $v_t(t)$. The PV source is connected to the DC link of the inverter with a capacitor C_{dc} . According to the instantaneous power definition, $v_t(t)$ and $v_c(t)$ are respectively the instantaneous PCC voltage and the inverter output voltage, then the average power of the PV denoted as $P(t)$, the apparent power $S(t)$ and the average reactive power $Q(t)$ of the PV system are given below [21]:

$$(3) \quad P(t) = \frac{V_t(t) \cdot V_c(t)}{\omega \cdot L_c} \cdot \sin \alpha$$

$$(4) \quad S(t) = V_t(t) \cdot I_c(t) = \frac{v_t(t)}{\omega L_c} \sqrt{V_t(t)^2 + V_c(t)^2 - 2V_t(t)V_c(t) \cdot \cos \alpha}$$

$$(5) \quad Q(t) = \sqrt{S^2(t) - P^2(t)} = \frac{V_t(t)}{\omega L_c} (V_c(t) \cdot \cos \alpha - V_t(t))$$

Where α , is the phase angle of $v_c(t)$ relative to the PCC voltage, we suppose that this angle value is very small ($\sin \alpha \approx \alpha$ and $\cos \alpha \approx 1$), then the two quantities $P(t)$ and $Q(t)$ can be approximated as shown in equations (6) and (7):

$$(6) \quad P(t) = \frac{V_t(t) \cdot V_c(t)}{\omega \cdot L_c} \cdot \alpha$$

$$(7) \quad Q(t) \approx \frac{V_t(t)}{\omega \cdot L_c} (V_c(t) - V_t(t))$$

In order to provide voltage and frequency (V-f) support to the grid, two controls are needed: a battery integrated V-F control and a battery integrated P-Q control which is the main purpose of the next paragraphs:

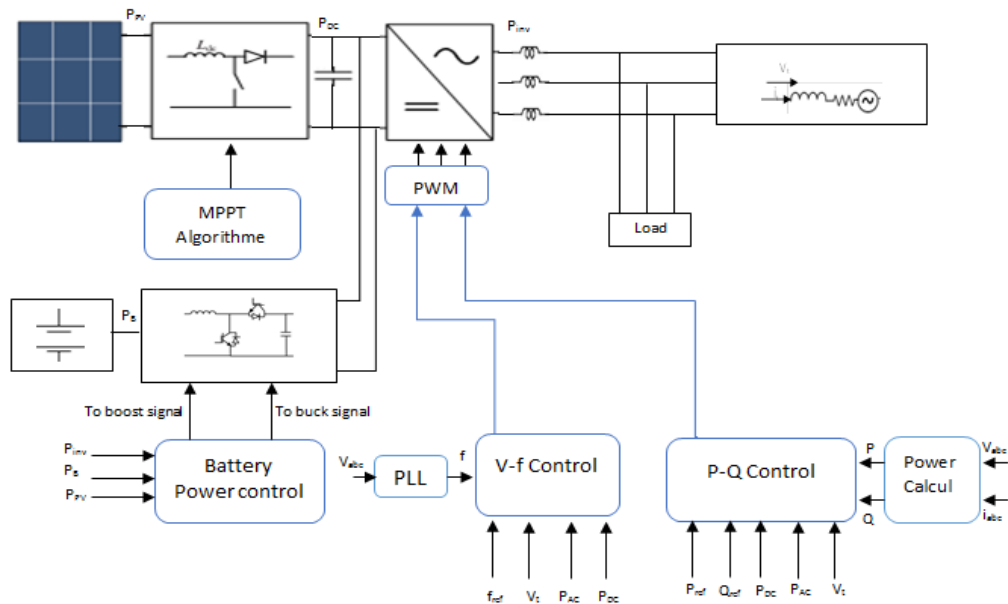


Fig. 4. System configuration of V-f and P-Q control of PV generator with battery storage

IV.1. Battery integrated V-F control

The battery and the V-f control diagrams are shown in Figures 5 and 6, respectively. The control consists of two different loops; one for V-f control at the inverter side and another loop for battery power management.

The control shown in Figure 5 describes the battery power control. The battery is connected in parallel with the PV system in order to supply or absorb active power and support the frequency control.

If there is enough solar power and the active power required for frequency control is less than PV MPP, then the battery will be charged. If there is not enough solar power available and if the active power required for frequency control is more than PV MPP, then the battery will be discharged and supply the deficit power in order to maintain the micro grid frequency at 60 Hz (conventional frequency used in this study).

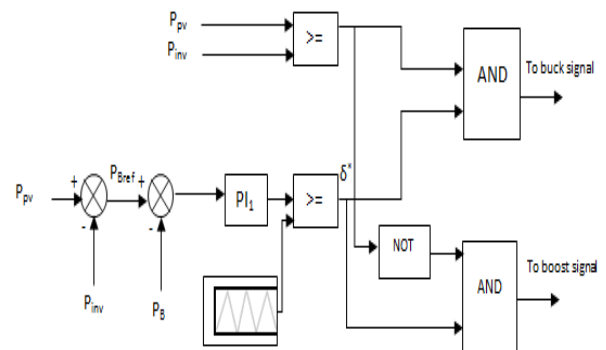


Fig. 5. Battery power control diagram

The reference power to the battery P_{battref} , is generated by subtracting the inverter active power injection P_{inverter} from the power generated by PV panel P_{pv} . The PI_1 controller receives the error signal obtained after subtracting the actual battery power P_{batt} , from the battery reference P_{battref} . Then we compare the obtained signal with a triangular waveform in order to generate the signal, δ^* . This is similar to common Pulse Width Modulation (PWM) in inverter controls. K_{P1} and K_{I1} are the proportional and integral gains respectively. The equation for this control is given by (8):

$$(8) \delta^* = K_{P1}(P_{\text{Battref}} - P_{\text{Batt}}) + K_{I1} \int_0^t (P_{\text{Battref}} - P_{\text{Batt}}) dt$$

In order to differentiate the charging and discharging mode of the battery, we need to compare P_{pv} with P_{inverter} . If $P_{\text{pv}} \geq P_{\text{inverter}}$, the battery is in charging mode, then, the signal obtained from the PWM, and the result of this comparison is passed through a logical AND to generate a switching signal which activates the Buck mode of the DC-DC converter. If $P_{\text{pv}} < P_{\text{inverter}}$ the opposite of this signal is passed through a logical AND to generate a switching signal which activates the Boost mode of the DC-DC converter.

Consequently, with this control loop, the bidirectional converter is capable of operating in both directions and ensures the charging and discharging state of the battery.

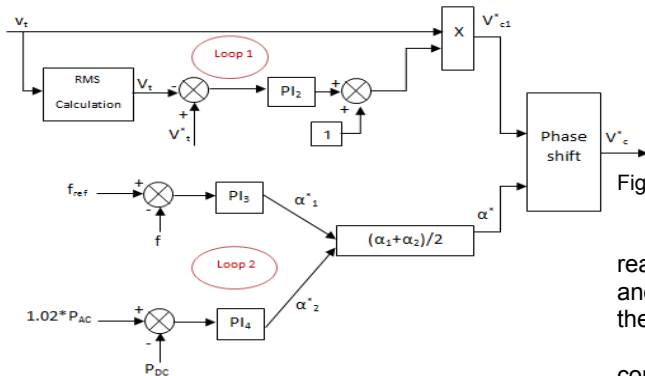


Fig. 6. V-f control diagram

As shown in the control diagram presented in Figure 6 (loop1), the PI_2 controller is used for controlling voltage at AC side. The voltage $v_t(t)$ is measured and its rms value V_t is calculated, then, this rms value is compared to a voltage reference and the error is fed to the PI_2 controller, 1 has been added to this control loop such that when there is no injection from the PV generator, the PV output voltage is exactly the same as the terminal voltage.

According to Figure 6 (loop 2), another feedback PI controller is used for controlling the active output power at the inverter side. The measured value is compared with the referenced micro grid frequency and this error is fed to the PI controller PI_3 that provides the phase shift contribution α^*_1 which shifts the voltage waveform in timescale such that the active power injected will be enough to maintain the frequency at 60Hz nominal value.

There is another controller used in the same loop 2. This controller ensures a balance of the active power between the AC and DC sides of the inverter. The measured AC side active power $P_{\text{ACmeasured}}$ is multiplied by a factor of 1.02 (considering the efficiency of inverter as 98%) then it's compared to DC side active power and the error is fed to

PI_4 to obtain the phase shift contribution from this loop α^*_2 . The two phases shift contributions from DC and AC sides α^*_1 and α^*_2 are then averaged as giving by equation 9 to obtain the final phase shift α^* which generates the voltage references signal v_c^* to control the inverter:

$$(9) \alpha^* = \frac{(\alpha^*_1 + \alpha^*_2)}{2}$$

Therefore, by controlling the DC side voltage and taking into account the phase-shift contributions from the DC and AC side active power, it can be assured that the active power at the DC and AC sides is balanced. This, coupled with the voltage control loop, ensures that the DC side voltage is maintained at the desired value by the AC side voltage.

IV.2. Battery integrated P-Q control

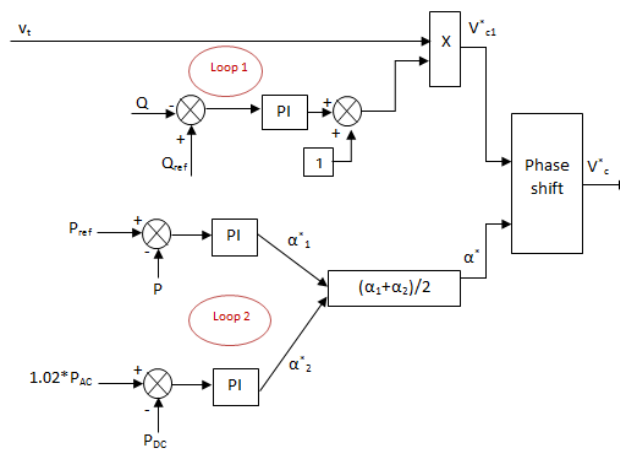


Fig. 7. Integrated Solar PV MPPT and P-Q control diagram

Figure 7 presents the proposed coordinated active and reactive power (P-Q) control integrated with PV systems and battery controls; it's the same as the one described in the previous section (4.1).

The first control loop (1) represents the reactive power control, the second one (loop 2) represents the active power control this loop also ensures the active power balance between the DC and AC sides of the inverter, and finally, the two phases shift obtained from this control loop are averaged such that the active power control at AC side and power balance objectives are taken into account.

V. Simulation results and discussion

The obtained simulations using Matlab/Simulink software are discussed in this section. The PV array delivers to the grid a maximum power of 100 kW at 1000 W/m² sun irradiance, the controller gains have been adjusted slightly in order to get the expected results.

V.1. Test of V-F Control

As is shown in Figure 8(a), when a high load is added to the studied system (60 Kvar), the PV array become unable to support the micro grid frequency, for this reason, it initially dips to a value of 58.9 Hz, similarly with the RMS value of output voltage, as it shown in figure 8(b), it initially dips to a value of 19,2 kV, which means that the studied system become unable to support the additional load, however, at 0.7 sec, the V-f control starts and then after some fluctuations it regulates the frequency back to 60 Hz and the voltage to 20kV, which confirm that the proposed control provide voltage and frequency (V-f) support to the grid.

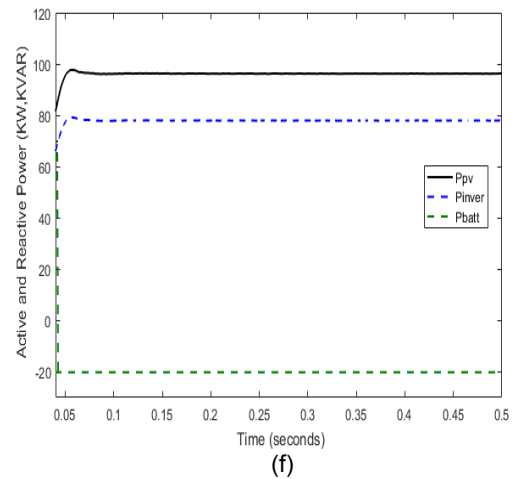
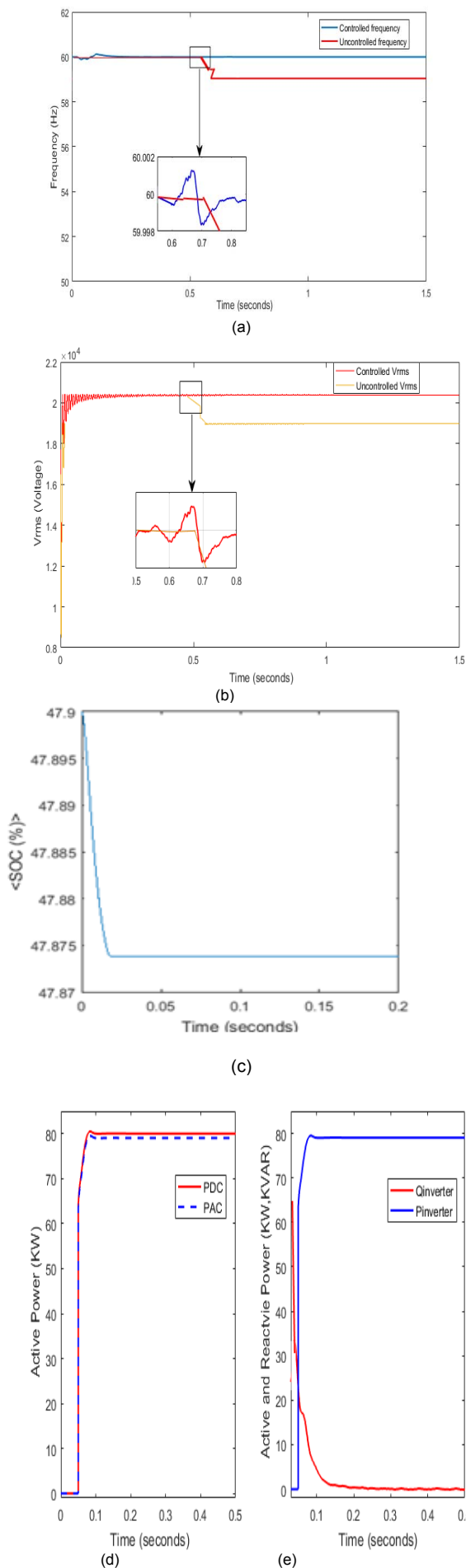


Fig. 8. Results of coordinated V-f control with solar PV including battery control

Figure 8(c) shows the battery state of charge (SOC), which shows that it gradually increases as the excess power is fed to charge the battery.

Figure 8(d) shows the active power at the DC and AC sides of the inverter. It is clear that the DC active power is slightly higher than the AC side three-phase average power due to some power losses between the DC and AC sides (taken as 3% in the present study). This power balance coupled with the AC side voltage control maintains the DC side voltage to a stable value.

Figure 8(e) shows the active and reactive power injection from the PV inverter that regulates the frequency and voltage of the micro grid. The active power injection from the inverter, which is required to maintain the frequency at 60 Hz, is around 80 kWh. However, there is a difference in the share of the PV generator and the battery energy storage while providing the required 80 kW to the micro grid.

This is evident from figure 8(f), which shows the active power from the PV, the battery, and the inverter, respectively. The PV generates the maximum power of 100 kW is more than is required to maintain the micro grid frequency. The surplus 20 kW is used to charge the battery. The negative sign in battery power means that it is a charging state (the battery absorbs power).

Therefore, the effectiveness of the proposed coordinated V-f control algorithm in micro grids is clearly demonstrates from the presented results.

V.2. Test of P-Q Control

Figure 9(a) shows the plot of active power from the PV generator, the inverter injection, and the battery power. As shown in the 1st curve, the power from PV is maintained constant at the MPP power of 100 kW. The active power injection from the inverter is maintained at the reference values of 50 kW. These reference values are demanded by the critical loads. The generation from PV is more than the critical load by 50 kW. Thus, this surplus power is sent to charge battery which is shown in the 3th curve of Figure 9(a). The negative sign of power from the battery shows that it is being charged.

Therefore, the power injection from the inverter comes only from the solar PV generator. (If we suppose that the critical load is greater than the PV generation at MPP, and then the surplus power will be supplied by the battery, in this case, the injection comes from PV and battery).

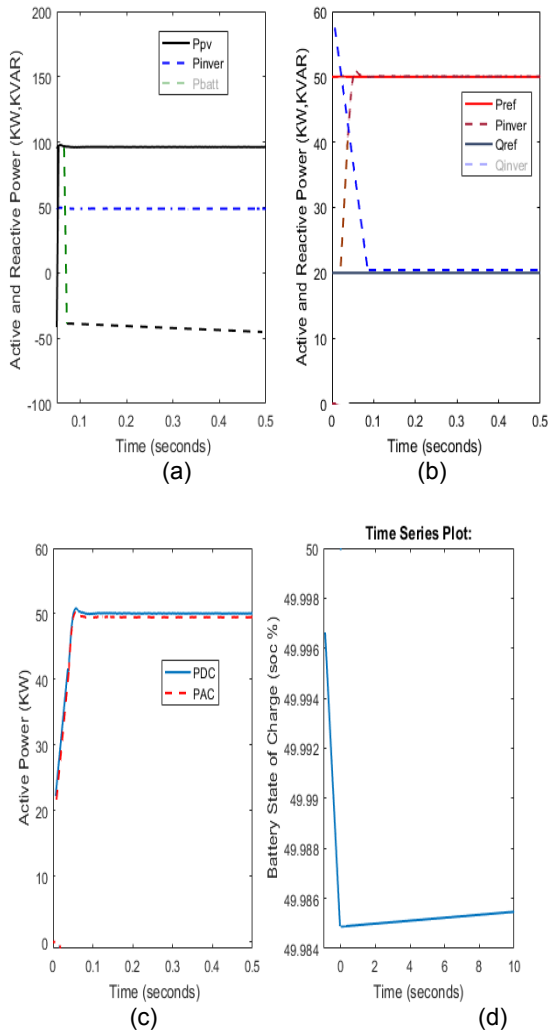


Fig. 9. Results of coordinated P-Q control with solar PV including battery control

Figure 9(b) shows the reference and actual active and reactive power of the PV inverter. The reference value of active power represents the critical loads of the micro grid as previously mentioned. The reference of the active power is 50 kW. Similarly, the reference of the reactive power is 20 KVAR. The references are chosen to demonstrate both charging and discharging the process of the backup battery energy storage system. It can be observed from Figure 9(b) that the proposed coordinated controls are capable of serving the critical loads.

Similarly, Figure 9(c) shows the active power measured at the DC and AC sides of the inverter. It is clear that the DC active power is slightly higher than the AC side three-phase average power.

Figure 9(d) shows the SOC of the battery. It is clear that the SOC increases as expected because of the charging scenario. It also validates the effectiveness of the battery control algorithm.

Consequently, the effectiveness of the proposed coordinated P-Q control algorithm in micro grids is clearly demonstrates from the presented results.

VI. Conclusion

This paper presents coordinated strategies of V-f and P-Q control of photovoltaic system connected to grid with the maximum power point tracking and the battery storage control in order to provide voltage and frequency support to

the grid and to maintain active and reactive power control instead of a high load addition. After the modelling of the grid connected PV systems with V-f and P-Q control, the obtained results are very important and satisfactory.

Simulations results show that when a high load is added to the studied system, the PV array become unable to support the micro grid frequency but the proposed control quickly regulates the frequency back to 60 Hz and the voltage to 20 kV, moreover, the power balance coupled with the AC side voltage control maintains the DC side voltage to a stable value, hence, PV and battery installations might be applied effectively to restore the micro grid frequency after disturbances, likewise, the proposed coordinated P-Q control algorithm can be effectively used in supplying some critical loads of a micro grid with solar PV and battery storage system.

In the present methods, the control parameters are dependent upon the PV, battery, and external grid conditions and must be modified with the changing conditions. The adaptive control methods could be a very useful and promising future direction of this work.

Appendix

Table 1. Photovoltaic parameters

Temperature	T	25	°C
Open circuit voltage	V_{oc}	64.2	V
Short circuit current	I_{sc}	5.96	A
Voltage, maximum power	V_{max}	54.7	V
Current, maximum power	I_{max}	5.58	A
Maximum power	P_{max}	305	W

Authors.

Essaghir soukaina: Ph.Student. in electrical engineering at National School of Applied Sciences Khouribga, Sultan Moulay Slimane University. Khouribga, 1, SAID HAJJI, Street, LAYMOUNE neighborhood, Morocco. E-mail: essaghirsoukaina@gmail.com

Benchagra Mohamed: Prof. department of Mechatronics at Superior School of Technology, Moulay Slimane University, Mghila, BP 591, Béni-mellal, Morocco, E-mail: m.benchagra@gmail.com

El barbri noureddine: Prof. department of Electrical Engineering at National School of Application Sciences Khouribga, Sultan Moulay Slimane University, Béni Amir, BP 77, Khouribga, Morocco, E-mail: elbarbri.noureddine@yahoo.fr

REFERENCES

- [1] L. Baoqi, Z. Yanhu, H. Bing, X. Liying and W. Zhao "An integrated control strategy of PV-battery hybrid systems," in *International Power Electronics and Application Conference and Exposition, PEAC 2104*, pp. 419–422.
- [2] C. K. Sao and P. W. Lehn, "Control and power management of converter fed micro grids," *IEEE Trans. Power Syst.*, vol. 23, no. 3, pp. 1088–1098, 2008.
- [3] "ESA – Energy Storage Association," 2016. [Online], available: www.energystorage.org.
- [4] S. Sieling, J. Welsch and H-J. Allien "Modeling and evaluation of combined photovoltaic-battery systems in the decentralized German power generation" in *International Conference Renewable Energy Research and Application, ICRERA*, pp. 770–775.
- [5] L. D. Watson and J. W. Kimball, "Frequency regulation of a micro grid using solar power," in *Twenty-Sixth Annual IEEE Applied Power Electronics Conference and Exposition (APEC)* April 2011, pp. 321–326, 2011.
- [6] S. Adhikari, L. Fangxing, "Coordinated V-f and P-Q control of solar photovoltaic generators with MPPT and battery storage in micro grids," *IEEE Trans. Smart Grid*, vol. 5, no. 3, pp. 1270–1281, 2014.
- [7] T. Ota, K. Mizuno, K. Yukita, H. Nakano, Y. Goto and K. Ichiyanagi, "Study of load frequency control for a microgrid," in *Australasian Universities Power Engineering Conference, AUPEC 2007*, pp. 1–6.

- [8] A.H. Mollah, G.K.Panda and P. K. Saha , "Three Phase Grid Connected Photovoltaic System with Maximum Power Point Tracking," in *International Journal of Advanced Research in Electrical, Electronics and Instrumentation Engineering.*, vol. 4, no. 5, p. ISSN (Online): 2278 – 8875.
- [9] A. Sayal, P.C. Sekhar and S. Mishra "A Review on Maximum Power Point Tracking Techniques for Photovoltaic Power Generating Systems," in *National Electrical Engineering Conference on Power and Energy Systems for Tomorrow, NEEC-2011*.
- [10] T. Laagoubi, M. Bouzi, and M. Benchagra, "Analysis and comparison of MPPT nonlinear controllers for PV system," in *International Renewable and Sustainable Energy Conference (IRSEC), 2015*.
- [11] T. Nguyen, A. Luo, "Multifunction converter based on Lyapunov function used in a photovoltaic system," *Turkish Journal of Electrical Engineering and Computer Sciences* vol. 22, no. 4, pp. 893–908, 2014.
- [12] A. Almula, G. M. Gebreel, "Simulation and Implementation of Two- Level and Three-Level Inverters By Matlab and Rt-Lab," MSc Thesis, p. 155, 2011.
- [13] H. Ouatman, M. Moussaid, M. Cherkaoui "Modeling and Control of a Grid-Connected PV Energy Conversion System," vol. 10, pp. 484–492, 2015.
- [14] S. Juing-Huei, C. Chao-Liang, C. Jiann-Jong and W. Chien-Ming, "SIMULINK behavior models for dc-dc switching converter circuits using PWM control ICs," *Int. J. Eng.*, vol. 22, no. 2, pp. 315–322, 2006.
- [15] C. F. Silva, J. M. Ferreira De Jesus, "A Model of a Battery Energy Storage System for Power Systems Stability Studies," pp. 1–8.
- [16] S. Hussain Basha, P. Venkatesh, "Control of Solar Photovoltaic (Pv) Power Generation in Grid-Connected and Islanded Microgrids," *Int. J. Eng. Reseaerch Gen. Sci.*, vol. 3, no. 3, pp. 121–141, 2015.
- [17] S. Essaghir, M.Benchagra, N. El Barbri, "Power factor control of a photovoltaic system connected to grid under load variation," in *International Conference on Electrical and Information Technologies (ICEIT), 2017*.
- [18] S. Essaghir, M.Benchagra and N. El Barbri, "Comparison between PI and PR Current Controllers of a Grid- Connected Photovoltaic System Under Load Variation," *IJPEDS*, vol. 9, N°3.
- [19] O. Tremblay, Louis-A. Dessaint, "Experimental validation of a battery dynamic model for EV applications," *World Electric Vehicle Journal*, vol. 3, no. 2, pp. 289–298, 2009.
- [20] M. Vojtek, M. Kolcun, Z. Čonka, and M. Mikita, "Cooperation of a Photovoltaic Power Plant With a Battery Energy Storage System," *Power Electr. Eng.*, vol. 33, pp. 35–39, 2016.
- [21] Y. Xu *et al.*, "Instantaneous Active and Nonactive Power Control of Distributed Energy Resources with a Current Limiter," *Energy Conversion Congress and Exposition, 2010*, pp. 3855–3861.